Design and Fabrication of Novel Polymeric Biodegradable Stents for Small Caliber Blood Vessels by Computer-aided Wet-spinning.

D. Puppi[1^], A. Pirosa[1^], G. Lupi[2], P.A. Erba[3], G. Giachi[4] and F. Chiellini[1*]

[1]BIOLab Research Group, Department of Chemistry and Industrial Chemistry, University of Pisa, UdR INSTM Pisa, via Moruzzi 13, 56124, Pisa, Italy
[2] Section of Neurosurgery, Department of Neuroscience, Pisa University Hospital, Pisa, Italy
[3]Department of Translational Research and New Surgical and Medical Technologies, University of Pisa, Via Savi 10, 56126 Pisa, Italy
[4] Ecopol SpA, Via Nuvolari 31, 55012 Capannori, Lucca, Italy

[^] These authors contributed equally to the work

* *Corresponding author:* Federica Chiellini, BIOLab Research Group, Department of Chemistry and Industrial Chemistry, University of Pisa, UdR INSTM Pisa
e-mail: federica.chiellini@unipi.it

Abstract. Biodegradable stents have emerged as one of the most promising approaches in obstructive cardiovascular disease treatment due to their potential in providing mechanical support while it is needed and then leaving behind only the healed natural vessel. The aim of this study was to develop polymeric biodegradable stents for application in small caliber blood vessels. Poly[(R)-3-hydroxybutyrate-*co*-(R)-3-hydroxyhexanoate], a renewable microbial aliphatic polyester, and poly(ε-caprolactone), a synthetic polyester approved by Food and Drug Administration for different biomedical applications, were investigated as suitable polymers for stent development. A novel manufacturing approach based on computer-aided wet-spinning of a polymeric solution was developed to fabricate polymeric stents. By tuning the fabrication parameters, it was possible to develop stents with different morphological characteristics (e.g. pore size and wall thickness). Thermal analysis results suggested that material processing did not cause changes in the molecular structure of the polymers. PHBHHx stents demonstrated great radial elasticity while PCL stents showed higher axial and radial mechanical strength. The developed stents resulted able to sustain human umbilical vein endothelial cells proliferation within two weeks of *in vitro* culture and they showed excellent results in terms of thromboresistivity when in contact with human blood.

Keywords: biodegradable stents, poly(hydroxyalkanoate)s, poly[(R)-3-hydroxybutyrate-*co*-(R)-3-hydroxyhexanoate], polycaprolactone, wet-spinning.

Introduction

The introduction of permanent metallic stents was a major advance over balloon angioplasty in the treatment of artery diseases, being highly effective in preventing acute vessel closure due to balloon-induced dissection, and in reducing the rate of restenosis [1]. However, it has been suggested that the role of the stent is temporary and limited to the intervention and shortly thereafter, until healing and re-endothelialization of the vessel wall is achieved [2]. In fact, after 6 months arterial remodeling typically enters a stable phase where no substantial scaffolding is needed any longer to prevent recoil [3]. Afterwards, the presence of a permanent stent, besides requiring a lifelong anticoagulant therapy, can lead to late thrombosis and chronic inflammation, and can hinder the lumen expansion associated with late vessel remodeling. Biodegradable stents have therefore emerged as one of the most promising approaches in obstructive cardiovascular disease treatment due to their potential in providing mechanical support while it is needed and then, once they are bioabsorbed, leaving behind only the healed natural vessel. This would allow the restoration of vasoreactivity and possibly vessel remodeling as well as to avoid the aforementioned concerns related with the presence of a permanent metallic implant [2]. In addition, biodegradable stents are particularly needed in

the case of pediatric cardiovascular treatments where a permanent stent usually requires a second surgery since the target vessel grows with child [3].

A number of biodegradable stents made of metallic or polymeric materials have been investigated over the last years [4, 5]. Mg alloys are by far the most investigated biodegradable metallic materials for intravascular stent development [6, 7]. The first metallic bioabsorbable stent implanted in humans was the Mg alloy stent studied in the "Clinical Performance and Angiographic Results of Coronary Stenting with Absorbable Metal Stents" trial [8]. Aliphatic polyesters, such as poly(L-lactic acid) (PLLA), poly(glycolic acid) (PGA), poly(D,L-lactic-co-glycolic acid) (PLGA), and poly(ε-caprolactone) (PCL), have been widely investigated for biodegradable stents development due to their relatively long degradation rate and suitable mechanical properties [5, 9]. The Igaki-Tamai stent (Kyoto Medical Planning, Japan), the first biodegradable stent implanted in humans, consists of an extruded high molecular weight PLLA filament with a zig-zag helical coil design [10]. The stent received the CE marking in 2007 for the treatment of peripheral artery diseases, and recent clinical outcomes showed its long term safety as coronary scaffold that could disappear within 3 years [11].The ABSORB Bioresorbable Vascular Scaffold based on PLLA (Abbott Vascular, CA) was the first bioabsorbable drug-eluting stent to have clinical outcomes similar to those following metallic drug-eluting stent implantation [12]. Other biodegradable stents that are currently under clinical investigation are the REVA Medical stent made of tyrosine polycarbonate (REVA Medical Inc., CA), the IDEAL stent made of a polyanhydride and salicylic acid (Bioabsorbable Therapeutics Inc, CA), and the novolimus-loaded DESOlve stent made of PLLA (Elixir Medical Corporation, CA) [8, 9].

Polymeric stents are generally composed by interconnected tubular elements with a zigzag or sinusoidal structure. They are fabricated starting from a tubular body, obtained by injection molding or melt extrusion, whose wall is made porous by means of selective material removal through laser ablation, mechanical machining or chemical etching [3]. Alternatively, polymeric stents are made through melt extrusion of a monofilament that is then woven into a braid-like embodiment. Flege *et al*. [13] recently reported on the development of stents made of PLLA or PLLA-*co*-PCL by means of a Selective Laser Melting technique. As highlighted by the authors, an additive manufacturing (AM) approach to stents fabrication allows achieving superior freedom in structural design and mechanical performance in comparison to conventional fabrication techniques. In fact, AM techniques allow fabrication of 3D objects with a predefined composition, geometry and size as well as a porous architecture characterized by a fully interconnected network of pores with customizable size, shape and distribution [14].

Wet-spinning is a polymeric fibers fabrication technique based on a non-solvent induced phase separation process, which involves the extrusion of a polymeric solution into a coagulation bath [15]. The application of AM principles to wet-spinning has enabled to develop 3D polymeric constructs with customized macro- and microstructural features. A number of studies have reported on the development of a novel computer-aided wet-spinning (CAWS) technique for the layered manufacturing of 3D porous polymeric constructs investigated as scaffolds for tissue engineering or *in vitro* 3D tissue modeling [16-24]. In particular, the CAWS technique has been recently employed for the development of a set of layered structures made of biodegradable polyesters of natural or synthetic origin, i.e. poly[(R)-3-hydroxybutyrate-*co*-(R)-3-hydroxyhexanoate)] (PHBHHx) [18, 24] and poly(ε-caprolactone) (PCL) [16, 21]. PHBHHx is a renewable microbial aliphatic polyester investigated for bone [18] and vascular [25] tissue engineering thanks to its biocompatibility and biodegradability as well as its better ductility and processing properties in comparison to other polyhydroxyalkanoates [26]. PCL is a synthetic aliphatic polyester approved by the Food and Drug Administration for various biomedical applications due to its well-assessed biocompatibility and biodegradability [27]. In addition, thanks to its good rheological and viscoelastic properties, PCL has been processed into a wide range of micro- and nano-scaled porous constructs investigated as biomedical implants [28].

The aim of this work was the development of PHBHHx and PCL tubular constructs as potential biodegradable stents for the treatment of small caliber blood vessels. For this purpose, a novel CAWS approach for the layered manufacturing of 3D microstructured polymeric constructs with a tubular geometry was developed. The processing parameters for the production of stents with different structural features were optimized and the developed prototypal samples were characterized for their morphological, thermal and mechanical properties. *In vitro* cell culture and hemocompatibility experiments were carried out to study the ability of the developed stents to support the adhesion and proliferation of endothelial cells and to avoid thrombus generation when in contact with blood.

Materials and Methods

Materials

Poly[(R)-3-hydroxybutyrate-*co*-(R)-3-hydroxyhexanoate)] (PHBHHx, 12 mol% HHx, Mw = 300000 g/mol) was kindly supplied by Tsinghua University (Beijing, China). PHBHHx was purified before use according to the following procedure: (a) the polymer was dissolved in 1,4 dioxane (5 % w/v) under stirring at room temperature for 1 h; (b) the solution was centrifuged at 4000 rpm for 1 h; (c) the supernatant was slowly dropped into 10-fold volume water; (d) after precipitation, the polymer was collected by filtering; (e) the polymer was washed with deionized water and then ethanol, finally vacuum dried and stored in a desiccator. Poly(ε-caprolactone) (PCL, CAPA 6800, Mw = 80000 g/mol) was supplied by Perstorp UK Ltd (Warrington, Cheshire, UK) and used as received. Chloroform, acetone and ethanol were purchased from Sigma Aldrich (Italy) and used as received.

Stents design and fabrication

PHBHHx was dissolved in chloroform under stirring for 2 h at 30 °C, while PCL was dissolved in acetone under stirring for 2 h at 35 °C to obtain homogeneous solutions at the desired concentrations. For the preparation of PHBHHx and PCL stents, a polymeric solution was placed into a glass syringe connected to a blunt tip stainless steel needle through a plastic tube. By using a programmable syringe pump (KDS100, KD Scientific, MA, USA), the solution was extruded at a controlled feeding rate directly onto a rotating mandrel immersed in an ethanol bath. The X-Y movement of the needle and the mandrel rotational velocity were controlled by an in-house made computer-controlled system. 3D tubular constructs were fabricated by winding the coagulating wet-spun polymeric fiber around the mandrel with a predefined layer-by-layer pattern (figure 1).

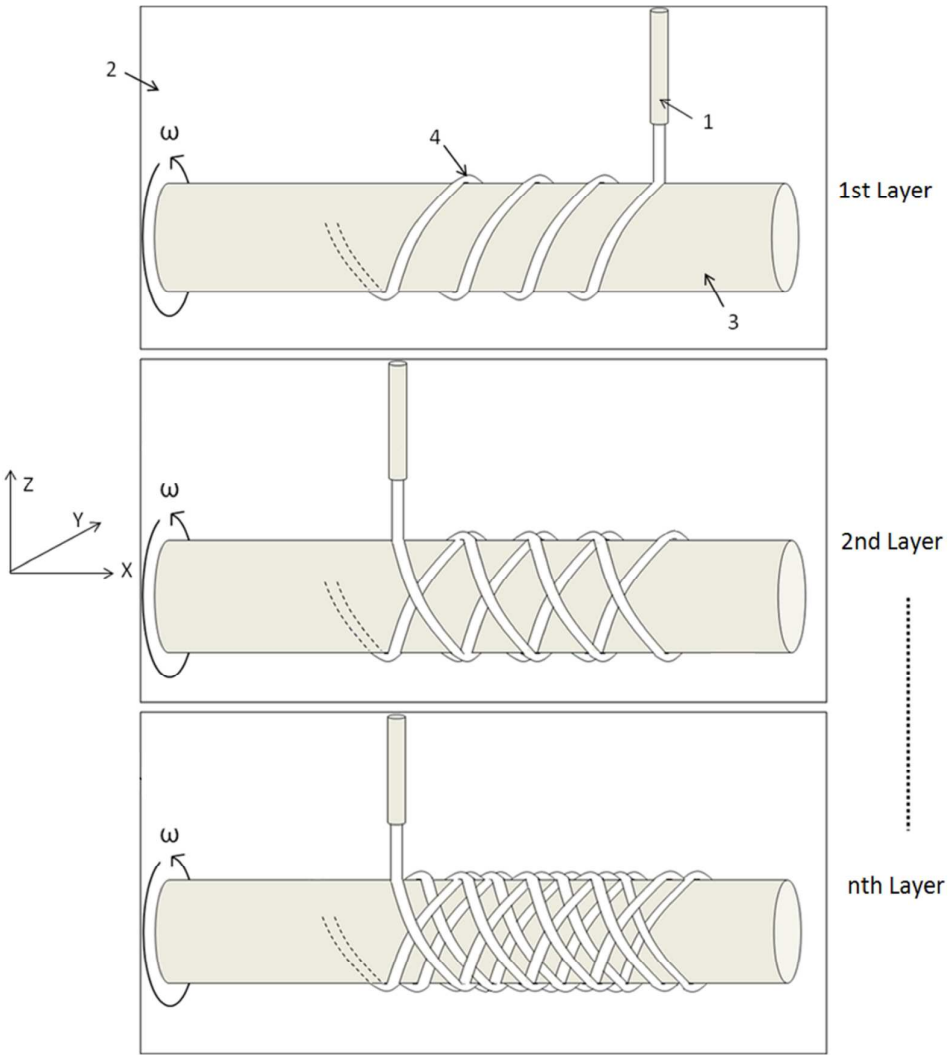

Figure 1. Schematics of CAWS approach for the layered manufacturing of polymeric stents: (1) extrusion needle, (2) coagulation bath, (3) rotating mandrel, (4) coagulating fiber.

The solvent/non-solvent systems optimized in previous studies regarding the wet-spinning of PHBHHx (chloroform/ethanol) and PCL (acetone/ethanol) [16, 18] were adopted.
A cylinder connected to a stepper motor was employed as rotating mandrel. A CAWS apparatus composed by an in-house modified subtractive Rapid Prototyping system (MDX-40A; ROLAND DG Mid Europe Srl, Ancona, Italy) equipped with a syringe pump (NE-1000; New Era Pump Systems Inc., Wantagh, NY, USA) [17] was employed to control the one directional translation of the extruding needle above the rotating cylinder. Customized translation patterns were written in G-code and uploaded into the equipment through the software Vpanel for MDX-40A. Fabrication process feasibility was tested at a prototyping stage with a simplified stent design resulting from overlapped layers of a fiber wound with a constant angle, as depicted in Figure 1. The effect of different processing parameters, such as polymer concentration (C), solution feed rate (F_R), distance between needle tip and mandrel (Z), needle inner diameter (D_N), needle translational velocity (V_T), mandrel rotational velocity (V_R) and number of winding layers (N_L) were systematically investigated in order the define a set of optimized processing parameters. The parameters employed for the fabrication of PHBHHx and PCL stent prototypes submitted to characterization are reported in Table 1. The prepared stents were left under a fume hood at room temperature for 24 h and subsequently vacuum-dried to remove any residual solvent.

Table 1: Optimized processing parameters for the production of PHBHHx and PCL stents with different NL (6, 8, 10 or 12).

Stent	C (% w/v)	F_R (mL/h)	Z (mm)	V_T (mm/min)	V_R (rpm)	D_N (mm)	Mandrel diameter (mm)	Mandrel material
PHBHHx	25	0.2	1	50	15	0.3	2	Teflon
PCL	20	0.4	2	50	15	0.3	2	Brass

C: Polymer concentration, F_R: solution feed rate, Z: needle tip-mandrel distance, D_N: needle diameter, V_T: needle translational velocity, V_R: mandrel rotational velocity.

Morphological analysis
Stents morphology was analyzed using Scanning Electron Microscopy (SEM, JEOL LSM 5600LV, Tokyo, Japan) under backscattered electron imaging. The stent structural parameters were measured by means of ImageJ 1.43u software (National Institutes of Health, Bethesda, MD, USA) on SEM micrographs with 35× magnification. By considering stent pores as rhombus-shaped, the two diagonals (d_1 and d_2) were measured as representative pore sizes. The fiber diameter (d_F) was defined as the stent strut thickness. The winding angle (W_A) was defined as the angle between the fiber direction and the axis of the rotating collector. Data were calculated over 20 measurements per scaffold.

Thermal characterization
Thermogravimetric analysis (TGA) was carried out using a TGA Q500 instrument (TA Instruments, Italy) in the temperature range 30 – 400 °C for PHBHHx samples and 30 – 600 ºC for PCL samples, at a heating rate of 10 ºC/min and under a nitrogen flow of 60 mL/min. The degradation temperature (T_{deg}) was evaluated as the temperature corresponding to a percentage weight loss of 2 %. Differential scanning calorimetry (DSC) analysis was performed at a heating rate of 10 ºC/min, cooling rate of 20 °C/min and under a nitrogen flow rate of 80 mL/min, using a Mettler DSC-822E instrument (Mettler Toledo, Italy). PHBHHx samples were analyzed in the range -40 to 180 ºC, while PCL samples in the range -100 to 100 ºC. The glass transition temperature (T_g) was evaluated by analyzing the inflection point, the melting temperature (T_m) and the crystallinity degree (C%) by analyzing the endothermic peaks in the heating scans. The second endothermic peak of PHBHHx termograms was considered to determine the T_m. Three samples for each kind of scaffold were tested in both thermal analyses.

Mechanical characterization
Mechanical properties of both PHBHHx and PCL stents were evaluated under either axial or radial compression using a DMTA V machine (Rheometric Scientific, Germany). Five specimens for each kind of stent were characterized in each test at a strain rate of 1 %/s until a maximum strain of 80 % [29]. Tubular

samples were placed between two parallel plates and tested under either axial or radial compression. The reaction force (F) was defined as the measured force, whilst the strain (ε) was evaluated as the ratio between the stent length/diameter variation (ΔL) and its initial length/diameter (L), for axial/radial compression, respectively. In order to evaluate the ability of the developed stents to recover their initial length/diameter when subjected to a load, a strain rate of 1 %/s was applied up to a given strain and then the load was released. The recovered length/diameter (for axial or radial compression, respectively) of the sample (L_E) was measured. The measurement was repeated for increasing values of strain in the range 5 – 80 %. Initial length/diameter recovery (L_R) was calculated as the percentage ratio between L_E and L at the end of each load. Elasticity retention strain (ε_{ER}) was defined as the highest applied strain corresponding to a $L_R \geq 95$ %. Elasticity retention force (F_{ER}) was determined as the reaction force corresponding to ε_{ER}.

In vitro biological characterization

Sterilization and NaOH treatment. PHBHHx and PCL stents were sterilized under ultraviolet (UV) light for 30 min. After sterilization, a set of stents was treated with 1.5 M NaOH for 90 min, in order to improve the surface hydrophilicity [30]. Samples were then extensively washed with sterile deionized water and incubated overnight with a solution of phosphate buffer saline (PBS) 1X containing penicillin/streptomycin (1 % v/v). Finally, samples were soaked with complete culture medium for 2 h at 37 °C in 5 % CO_2 before cell seeding.

Endothelial cell proliferation. Human umbilical vein endothelial cells (HUVEC), supplied by the Department of Translational Research and New Technology in Medicine, University of Pisa, were cultured as monolayer in M199 medium (Life Technologies, USA), supplemented with fetal bovine serum (20 % v/v), penicillin/streptomycin (1 % v/v), bFGF (5 ng/ml) and L-glutamine (4 mM). Confluent cells were trypsinized, detached from the flask and seeded on the stents placed in 96 wells plate, in a number of 1 x 10^4 and in final volume of 100 μl of complete culture medium. Cells were incubated at 37 °C in humidified atmosphere containing 5 % CO_2; cells grown on tissue culture polystyrene (TCPS) covered with gelatin (1 % w/v) were considered as control. HUVECs viability and proliferation were investigated by WST-1 tetrazolium salt reagent (Roche, Switzerland) at days 2, 7 and 14 after seeding, as previously reported [18]. Briefly, cells were incubated for 4 h with WST-1 reagent diluted 1:10, at 37 °C and 5 % CO_2. Measurements of formazan dye absorbance, which directly correlates with the number of viable cells, were carried out with a microplate reader (Biorad, USA) at 450 nm, using 655 nm as reference wavelength. Cell proliferation was expressed as percentage with respect to cells grown on gelatin covered TCPS.

Gravimetric analysis of the thrombus. Fresh human blood obtained from voluntary donors (Monovette, SARSTEDT with 3.8 % sodium citrate) was supplied by the Department of Translational Research and New Technology in Medicine, University of Pisa. NaOH treated and untreated stents were placed in eppendorf tubes, covered with 200 µl of anti-coagulated blood and incubated at 37 °C with 0.1 M $CaCl_2$ solution (20 µl) to activate blood coagulation. After 30 min of incubation in a closed chamber, the samples were rinsed with 0.15 M NaCl solution and fixed with paraformaldehyde (3.8 % w/v in PBS 1X). After 12 h of drying in a clean atmosphere, the weight of the thrombus formed on the stents was obtained by subtracting the initial weight of the stent. A glass tube was used as a positive control and the percentage of thrombus formation was calculated with respect to positive control. The assay was performed on triplicate samples for each material.

Statistical analysis

Quantitative data are presented as mean ± standard deviation. Data sets were analyzed using Student t-test, one-way analysis of variance (ANOVA) and *post hoc* Tukey test. Differences were considered statistically significant at a value of $p < 0.05$.

Results

Stents fabrication

Microstructured PHBHHx or PCL stents were fabricated by a novel CAWS approach involving the controlled winding of a coagulating polymeric fiber around a rotating mandrel that was immersed into a coagulation bath of ethanol. The synchronized motion of the translating solution feeding needle and the rotating mandrel allowed obtaining tubular 3D porous architectures by fabricating a specific number of

winding layers one on top of the other. Several processing parameters were investigated in order to optimize the fabrication process and the morphology of the fabricated stents in terms of length, inner diameter, wall thickness, wall microstructure, fiber diameter and fiber winding angle. For instance, by varying the number of wound fiber layers (N_L) or the mandrel rotational velocity (V_R), stents with different porosity and wall thickness were obtained. Representative pictures of optimized stents with different N_L (6, 8, 10 or 12), a designed inner diameter of 2 mm and a length of 5 mm are reported in figure 2. The most influent optimized processing parameters for stents fabrication are reported in table 1.

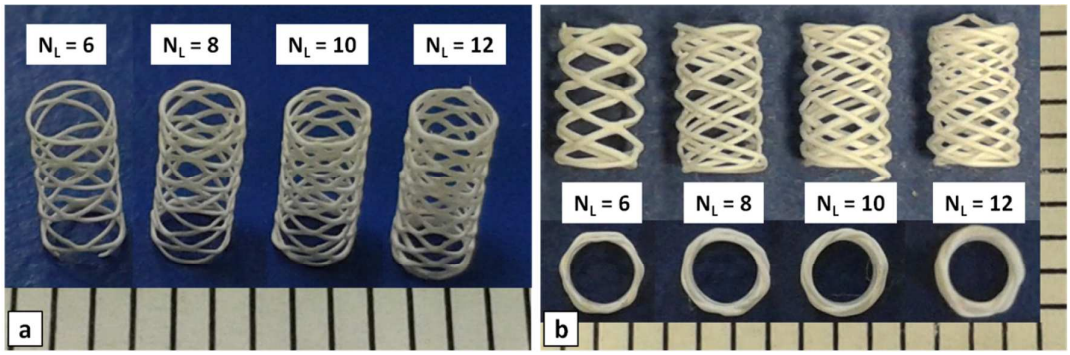

Figure 2. Representative pictures of PHBHHx (a) and PCL (b) stents with different N_L fabricated by employing a 2 mm rotating mandrel. Measure unit = 1 mm.

Morphological analysis

SEM analysis of the developed stents revealed that the wet-spun fibers constituting the two kinds of stent were characterized by a highly porous morphology (figure 3). Fusion at fiber-fiber contact points appears more pronounced in PHBHHx than in PCL stents.

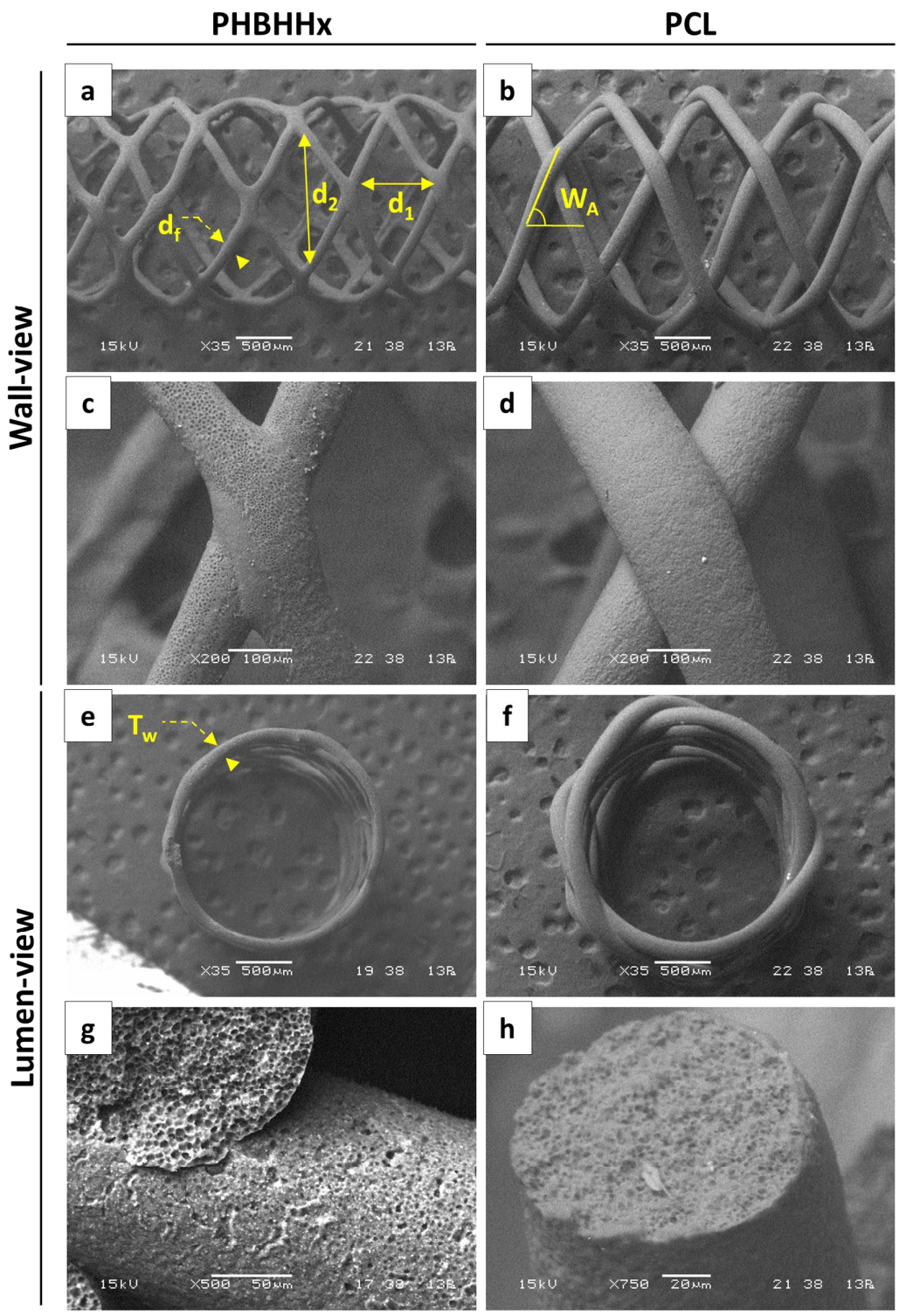

Figure 3. Representative SEM micrographs of side view (a)-(d), top view (e)-(f) and fiber cross-section details (g)-(h) of a PHBHHx stent with N_L = 8 and a PCL stent with N_L = 6.

Structural parameters analysis (Table 2) revealed that the developed stents were characterized by a fiber diameter (d_f) in the range 100-200 µm that was not affected by variations in N_L, while their wall thickness (T_W) and pore sizes (d_1 and d_2) could be varied in a certain range by acting on N_L. Due to their significantly smaller d_f and more pronounced fusion at crossing points, PHBHHx stents have significantly smaller T_W (80-180 µm) than PCL stents (180-350 µm). Significant differences in d_f and winding angle (W_A) between PHBHHx and PCL stents with the same N_L led to significantly different pore sizes that varied in the range of

hundreds of micrometers. For both kinds of stent, there were no significant changes in lumen diameter by varying N_L.

Table 2. Architectural parameters of PHBHHx and PCL stents

	Stent	Fiber diameter (d_f) (mm)	Winding angle (W_A) (°)	Wall thickness (T_W) (μm)**	d_1 pore size (mm)**	d_2 pore size (mm)**	Lumen diameter (mm)
N_L=6	PHBHHx	0.12±0.01*	54.1±2.8*	89±09*	0.83±0.10*	1.15±0.15*	1.79±0.06*
	PCL	0.17±0.02	63.7±6.5	218±35	0.73±0.07	1.44±0.15	1.88±0.04
N_L=8	PHBHHx	0.11±0.02*	56.5±2.7*	94±15*	0.67±0.09	1.09±0.09*	1.84±0.03
	PCL	0.13±0.01	64.6±2.5	228±32	0.55±0.07	1.18±0.10	1.86±0.05
N_L=10	PHBHHx	0.11±0.01*	56.5±2.7*	128±24*	0.43±0.06*	0.67±0.06*	1.79±0.03*
	PCL	0.14±0.02	64.6±2.5	288±68	0.36±0.05	0.89±0.09	1.87±0.02
N=12	PHBHHx	0.12±0.01*	58.0±6.0*	163±14*	0.34±0.05*	0.57±0.09	1.79±0.04*
	PCL	0.14±0.01	65.2±2.2	318±31	0.30±0.03	0.73±0.06	1.88±0.03

Data expressed as average ± standard deviation (n=20).
* For a given parameter, value significantly different to that of the PCL sample with the same N_L.
** For a given parameter, values of same kind of stent (PHBHHx or PCL) with different N_L are statistically different.

Thermal properties

TGA and DSC thermograms of raw materials and selected stent prototypes (PCL stent with N_L = 6 and PHBHHx stent with N_L = 8) are reported in figure 4.

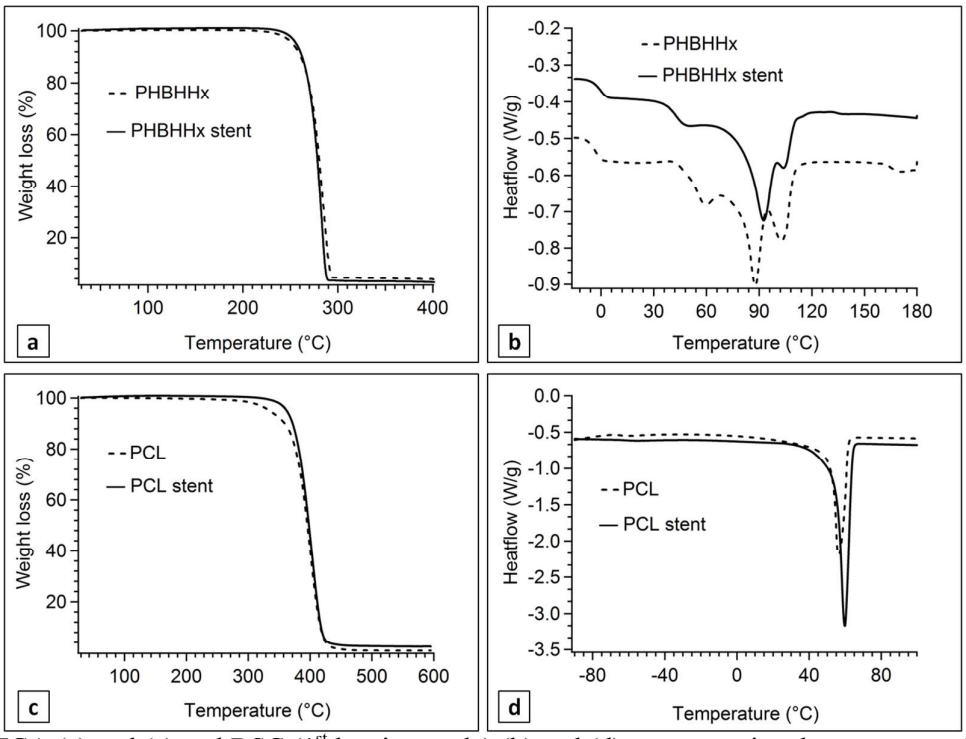

Figure 4. TGA (a) and (c) and DSC (1st heating cycle) (b) and (d) representative thermograms of PHBHHx and PCL stents, as compared to raw materials.

Both PHBHHX and PCL scaffolds were characterized by a TGA profile overlapping with those of unprocessed polymers with not statistically significant differences in thermal degradation temperature (T_{deg}). By analyzing the first heating DSC curves, it was evident that PCL thermograms were characterized by a single melting endotherm, while PHBHHX curves by three melting endotherms. In the second heating curves of PHBHHx samples only the glass transition was detectable. No statistically significant differences in terms of T_{deg}, glass transition temperature (T_g), melting temperature (T_m) and crystalline degree (C%) were found between unprocessed polymer (PHBHHx – raw) and PHBHHx stents (Table 3).

Table 3: Thermal properties of raw and processed materials obtained by TGA and DSC analyses.

Sample	T_{deg} (°C)	T_g (°C)		T_m (°C)		C%	
		1st heat.	2nd heat.	1st heating	2nd heating	1st heating	2nd heating
PHBHHx - raw	242.64 ± 3.65	-0.37±0.40	-0.62±0.46	88.74 ± 2.02	-	34.33 ± 1.95	-
PHBHHx - stent	249.80 ± 4.00	-0.42±0.26	-0.64±0.09	92.20 ± 0.42	-	33.03 ± 0.41	-
PCL – raw	354.61 ± 3.55	-62.41±0.88	-63.54±1.48	66.75 ± 2.00*	58.81 ± 3.60	72.59 ± 2.76**	60.15 ± 0.75
PCL – stent	350.24 ± 2.70	-	-62.94±1.02	59.69 ± 0.63*	55.63 ± 1.36	80.66 ± 1.89**	58.64 ± 0.21

Data expressed as average±standard deviation (n=3).
Values with the same number of * were significantly different ($p < 0.05$).

While no significant difference in T_{deg} was detected between PCL stents and raw PCL, PCL stents showed lower T_m and higher C% than raw material, as obtained from the first heating cycle analysis. However, by comparing data from the second scan, any significant difference in thermal parameters between raw PCL and PCL stents was detected.

Mechanical properties

Axial compression properties. Generally, the force/strain curves from axial compression characterization of PHBHHx and PCL stents with N_L from 6 to 12 (figure 5a and 5b) were characterized by an initial roughly linear region at low values of strain (up to ≈ 20 %) and reaction force (0.01 – 0.05 N for PHBHHx, 0.1 – 0.2 N for PCL). After around 20 % of strain, PHBHHx stents curves were characterized by a region in which the reaction force was in the range 0.02 – 0.05 N and then by a final high strain region characterized by a fast increase of the reaction force, that reached a maximum value in the range 0.09-0.33 N, depending on N_L. PCL stents curves showed a fast increase in reaction force after ≈ 20 % strain up to a maximum reaction force in the range 0.32-1.65 N, depending on N_L.

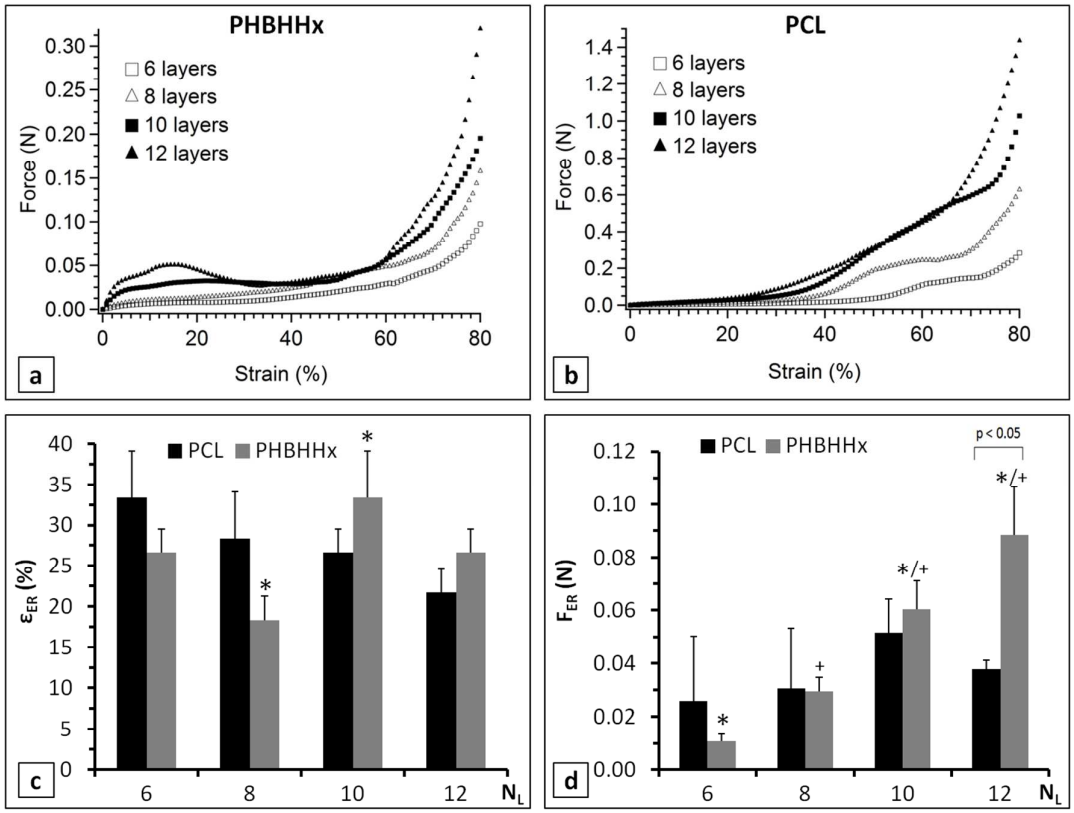

Figure 5. Representative axial compression stress-strain curves of PHBHHx (a) and PCL (b) stents (strain rate of 1 %/s, up to 80 % strain). Elasticity retention properties for axial compression of PHBHHx and PCL stents: (c) elasticity retention strain (ε_{ER}); (d) elasticity retention force (F_{ER}). Values with the same symbol (*, °, $^{+}$) were significantly different ($p < 0.05$).

Values of axial reaction force recorded at four representative values of strain are reported in table 4. At 10 % strain, PHBHHx and PCL stents did not show significant differences in terms of reaction force for $N_L = 6$ and $N_L = 8$, while for $N_L = 10$ and $N_L = 12$ PHBHHx stents showed higher reaction force than PCL stents. However, comparing the reaction forces at 30, 50 and 80 % of strain, PCL stents showed significantly higher values than the corresponding PHBHHx stents with the same N_L. Initial length recovery after 80 % strain test of PHBHHx stents was in the range 80 – 90 %, while that of PCL stents was in the range 45 – 70 %.

Table 4. Compressive axial reaction force (at 10, 30, 50 and 80 % strain) of PHBHHx and PCL stents with different (N_L in comparison to melt electrospun PCL and commercial metallic stents.

	Stent	Reaction Force (N)				Initial length recovery (%)[1]
		Axial strain=10%	Axial strain=30%	Axial strain=50%	Axial strain=80%	
$N_L = 6$	PHBHHx	0.005 ± 0.001	0.008 ± 0.001	0.013 ± 0.001	0.098 ± 0.026	88.12 ± 2.60
	PCL	0.004 ± 0.001	0.010 ± 0.001	0.037 ± 0.002	0.332 ± 0.070	66.38 ± 2.04
$N_L = 8$	PHBHHx	0.009 ± 0.001	0.014 ± 0.002	0.023 ± 0.004	0.144 ± 0.094	85.45 ± 6.94
	PCL	0.008 ± 0.001	0.022 ± 0.001	0.191 ± 0.008	0.582 ± 0.079	64.84 ± 2.75
$N_L = 10$	PHBHHx	0.024 ± 0.002	0.032 ± 0.002	0.029 ± 0.002	0.195 ± 0.076	89.46 ± 4.39
	PCL	0.015 ± 0.001	0.050 ± 0.001	0.309 ± 0.011	0.978 ± 0.137	55.70 ± 3.06
$N_L = 12$	PHBHHx	0.039 ± 0.006	0.037 ± 0.004	0.030 ± 0.014	0.320 ± 0.070	88.89 ± 3.98
	PCL	0.015 ± 0.001	0.087 ± 0.008	0.317 ± 0.015	1.328 ± 0.256	51.11 ± 6.70

Data expressed as average ± standard deviation (n=5).
[1] Percentage of initial length recovery after 80% axial strain

The developed stents were also tested to evaluate the maximum values of axial compressive strain and reaction force at which they recover elastically their initial height once the load is released (figure 5c and 5d). By increasing N_L of PHBHHx stents, the elasticity retention strain (ε_{ER}) was in the range 14 – 40 % and the corresponding reaction force (F_{ER}) increased significantly from 0.011 ± 0.003 N ($N_L = 6$) to 0.088 ± 0.018 N ($N_L = 12$). By increasing N_L, PCL stents were characterized by a slightly but not statistically significant decrease of ε_{ER} from 33.33 ± 5.77 % ($N_L = 6$) to 21.67 ± 2.89 % ($N_L = 12$), while F_{ER} was in the range 0.01 – 0.06 N. It is worth to notice that no significant differences of ε_{ER} and F_{ER} were seen between stents made of different materials but the same N_L (except for F_{ER} when $N_L = 12$).

Radial compression properties. The force-strain radial curves were characterized by an initial roughly linear region at low values of strain (below around 10 %) and reaction force (0.01 – 0.03 N for PHBHHx, 0.10 – 0.20 N for PCL), followed by a decrease of the curve's slope and a third region where the slope increased again by increasing the strain, until a maximum reaction force (80 % strain) in the range 0.06-0.30 N for PHBHHx and 0.62-1.12 N for PCL (figure 6).

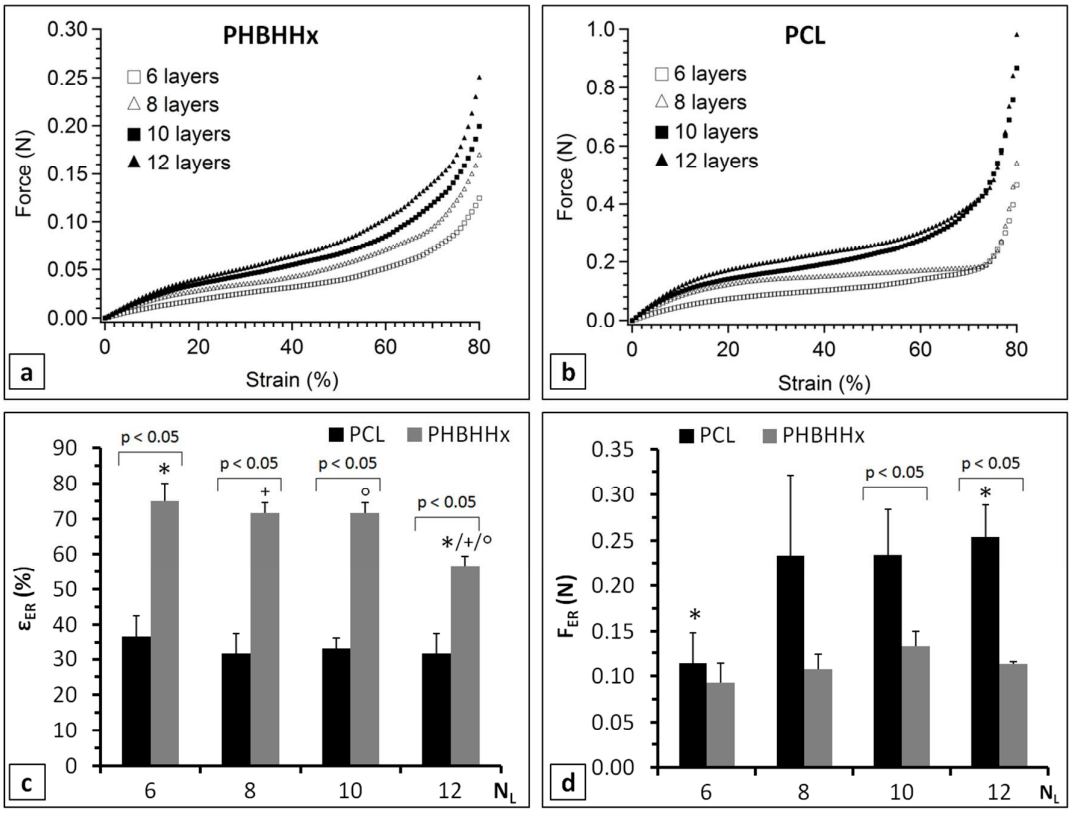

Figure 6. Representative radial compression stress-strain curves of PHBHHx (a) and PCL (b) stents (strain rate of 1 %/s, up to 80 % strain). Elasticity retention properties for radial compression of PHBHHx and PCL stents: (c) elasticity retention strain (ε_{ER}); (d) reaction force at elasticity retention strain (F_{ER}). Data are expressed as mean±standard deviation (n=3). Values with the same symbol (*, °, +) were significantly different ($p < 0.05$).

The force/strain relationship (reaction forces corresponding to four representative values of strain: 10 – 30 – 50 – 80 %) of PHBHHx and PCL stents with N_L from 6 to 12 are shown in Table 5. For the same N_L, PCL stents showed significantly higher radial reaction forces than PHBHHx stents at the selected values of strain. Initial diameter recovery at 80 % strain of PHBHHx stents was in the range 90 – 95 %, while that of PCL stents was in the range 65 – 80 %.

Table 5. Compressive radial reaction force (at 10, 30, 50 and 80 % strain) of PHBHHx and PCL stents with different N_L, in comparison to injection molded PCL stents and commercial metallic stents.

	Stent	Reaction Force (N)				Initial diameter recovery (%)[1]
		Diameter strain=10%	Diameter strain=30%	Diameter strain=50%	Diameter strain=80%	
$N_L = 6$	PHBHHx	0.011 ± 0.002	0.026 ± 0.001	0.039 ± 0.002	0.125 ± 0.064	93.50 ± 3.39
	PCL	0.049 ± 0.003	0.091 ± 0.001	0.117 ± 0.011	0.466 ± 0.146	75.22 ± 3.17
$N_L = 8$	PHBHHx	0.018 ± 0.002	0.035 ± 0.002	0.054 ± 0.004	0.170 ± 0.034	93.32 ± 1.48
	PCL	0.084 ± 0.003	0.140 ± 0.011	0.159 ± 0.012	0.540 ± 0.167	70.62 ± 7.30
$N_L = 10$	PHBHHx	0.022 ± 0.003	0.045 ± 0.002	0.067 ± 0.004	0.200 ± 0.031	93.95 ± 1.54
	PCL	0.100 ± 0.004	0.148 ± 0.011	0.228 ± 0.015	0.868 ± 0.263	74.76 ± 2.51
$N_L = 12$	PHBHHx	0.026 ± 0.002	0.051 ± 0.003	0.079 ± 0.011	0.250 ± 0.042	93.27 ± 1.71
	PCL	0.118 ± 0.007	0.201 ± 0.013	0.256 ± 0.019	0.980 ± 0.078	74.79 ± 1.02

Data expressed as average ± standard deviation (n=5).
[1] Percentage of initial diameter recovery after 80% axial strain

The developed stents were also tested to evaluate the maximum radial compressive strain and reaction force at which they recover their initial diameter once the load is released. As shown in Figure 6c and 6d, by increasing N_L, PHBHHx stents were characterized by a significant decrease of ε_{ER} from 75.00 ± 5.00 % (N_L = 6) to 56.67 ± 2.89 % (N_L = 12) while the corresponding F_{ER} values were in the range 0.07–0.15 N without significant differences among the different values. As for PCL stents, by increasing N_L ε_{ER} was in the range

31 – 34 % without significant differences, while F_{ER} increased significantly from 0.11 ± 0.03 N (N_L = 6) to 0.25 ± 0.03 N (N_L = 12). PHBHHx stents showed significantly higher ε_{ER} than PCL ones, but lower F_{ER} for N_L = 10 and N_L = 12.

In vitro preliminary biological evaluation

Cell viability and proliferation. HUVEC cell line was selected as a model for vascular endothelization. Preliminary biological investigations of the optimized PHBHHx (N_L = 8) and PCL (N_L = 6) stents, both plain and NaOH-treated, were carried out in order to evaluate their ability to sustain HUVEC cell adhesion and proliferation. All tested stents were able to sustain endothelial cell proliferation during the two weeks cell culture experiment (figure 7).

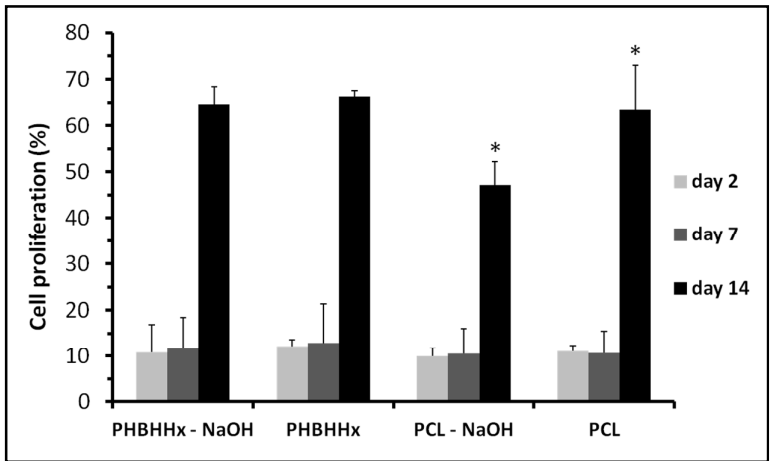

Figure 7. Cell proliferation of HUVECs cultured onto PHBHHx and PCL stents, evaluated by WST-1 assay. Values marked by * were significantly different ($p < 0.05$).

At the first two endpoints (days 2 and 7 of culture) all the samples were characterized by a slow cellular proliferation, while at day 14 a clear increase of HUVEC cell proliferation was detected for both materials and treatments. Regarding cell proliferation at day 14 on PCL stents, the increase measured on plain PCL samples was significantly higher than NaOH-treated PCL stents, whereas no significant differences were observed between NaOH-treated and plain PHBHHx stents.

Stents thrombogenicity evaluation. Thrombogenic effect of PHBHHx and PCL stents was investigated under static conditions by incubating the constructs with fresh human blood and compared to glass, selected as positive control. Overall, each typology of stents generated a relatively low amount of thrombus with respect to the control (Figure 8a). These visual observations were substantiated through the thrombus quantification studies by calculating the sample weight (Figure 8b). The results displayed a percentage weight of thrombi in the range between 5 – 12 % and a significantly lower thrombus deposition on NaOH-treated PHBHHx compared with NaOH-treated PCL stents. However, no significantly differences were detected between NaOH-treated and the analogous plain stents.

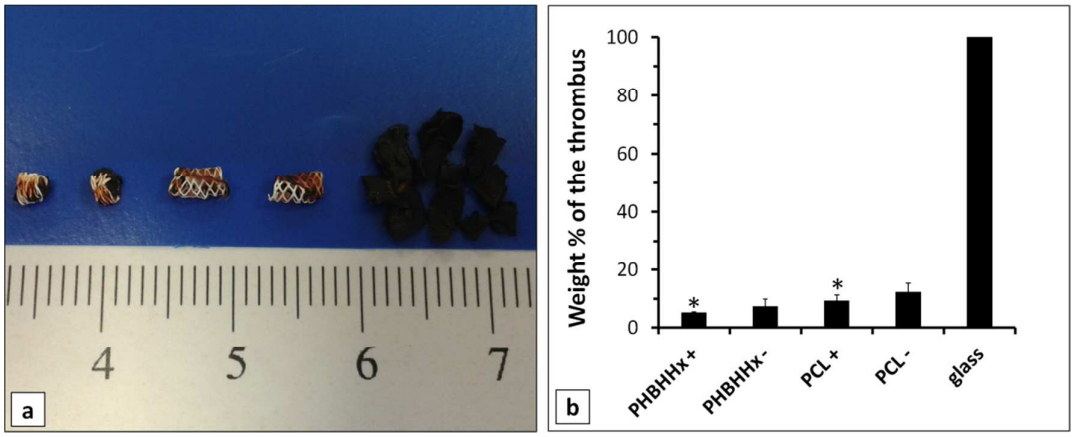

Figure 8. Gravimetric analysis of the thrombus: (a) representative picture of the thrombus formed in contact with the stents (from left to right: NaOH treated PHBHHx, plain PHBHHx, NaOH treated PCL, plain PCL, glass); (b) histogram of the weight % of the thrombus with respect to positive control; +/- indicates NaOH treatment presence/absence. Data are expressed as mean±standard deviation (n=3). Values marked by * were significantly different ($p < 0.05$).

Discussion

Different material processing techniques, such as centrifugal casting [31], dip coating [32], electrospinning [33] and injection molding [34], have been proposed in the past years to develop polymeric tubular structures investigated for various biomedical applications (e.g. nerve guides, vascular grafts and blood vessel engineering). In addition, recent studies focused on applying AM principles to the fabrication of polymeric tubular constructs. Alginate vascular-like tubes were successfully developed by using Inkjetting [35] or Laser-assisted Printing [36]. The aforementioned Selective Laser Melting technique application is a further successful example of polymeric tubular structures production by AM [37]. Melt electrospinning in a direct writing mode was also recently proposed as a suitable technique for the fabrication of biodegradable porous tubes through a continuous, layered winding of a melt electropsun microfiber around a roto-translating cylindrical collector [38, 39]. As shown by the reported results, that is a powerful approach to achieve an advanced control over the micro- and macroscopic architecture as well as the mechanical properties of the resulting tubular scaffolds. Similarly, the CAWS technique developed in this study, based on the controlled winding of a coagulating polymeric fiber around a rotating mandrel, allows to customize stent macro- and micro-structural features (e.g. wall thickness and porosity), by simply changing fabrication parameters such as the number of winding layers, the run length and the mandrel diameter. While the main advantages of the melt electrospinning writing technique are a high resolution of the structural elements (fiber diameter of tens down to few μm) and avoiding the use of organic solvents, CAWS is suited for processing a broader range of polymeric materials from natural and synthetic resources [15] as well as for loading the polymeric matrix with drugs by a direct solution blending method avoiding post-fabrication treatments, technological complexity and thermal processing that can cause denaturation of therapeutics [19].

According to the American Society for Testing Materials, AM refers to "the process of joining materials to make objects from 3D model data, usually layer upon layer, as opposed to subtractive manufacturing methodologies" [40]. The CAWS approach described in this study and the melt electrospinning writing technique reported in literature for tubular constructs fabrication could be seen both as falling within this generic definition upon the consideration that they are based on a computer-controlled layer-by-layer process. However, more specific definitions consider a complete digitalization and elimination of tools and dies as distinctive features of AM compared with other manufacturing processes [41]. Therefore, the suitability of these two techniques for polymeric tubes manufacturing in the absence of a mandrel should be assesed in order to fully qualify them as AM processes.

The main advantage of the CAWS approach over other techniques designed for the fabrication of polymeric stents and other polymeric tubular constructs (e.g. melt-extrusion fiber braiding, selective laser cutting and melt electrospinning writing) is represented by the possibility to endow the polymeric structure with a dual-level pore arrangement given by macropores with a size in the scale of hundreds of microns and a nano/microporosity of the wound fiber (Figure 3). Considering the controlled effect that various processing variables have on the spreading and size at different scale levels of the resulting pores network [42], this

approach represents a powerful tool to tune various key properties strictly related to stent porosity, such as the biodegradation rate, the release kinetics of loaded bioactive agents and the interaction with endothelial cells. For instance, the micro/nanoporous matrix morphology observed during SEM analysis (Figure 3) will result in markedly increased polymer-physiological medium interface area. In comparison to analogous stents with a dense polymeric matrix, such local porosity will likely lead to accellerated biodegradation of the two investigated polymers, which is governed by a hydrolytic chain scission mechanism that, especially for PCL, requires several months for complete material degradation *in vivo* [43, 44].

Being a process based on fiber extrusion, CAWS potentially presents a degree of freedom in stent desing comparable to that of melt-extruded fiber braiding techniques. However, relevant differences related to the deposition process performed in a liquid medium should be investigated by testing more complex designs than that selected in the prototyping stage carried out in this study. This is an important issue for future research considering that various stent properties, such as expandibility, mechanical response and hemodynamic compatibility, are highly dependent on the selected stent design.

Polymer fiber solidification during stent manufacturing by CAWS, as well as the morphology of the resulting fiber and the 3D porous network, are governed by a non-solvent induced phase inversion process. The solvent/non-solvent exchange in the coagulating solution filament lowers polymer solubility causing a separation of the solution into two phases with different composition. Under optimal composition of the extruded filament, a polymer-lean phase is dispersed into a continuous polymer-rich phase leading to the formation of a porous polymeric matrix [15]. A proper balance among the various processing parameters (e.g. polymer concentration, solution feed rate and distance between needle tip and mandrel surface) is necessary for the formation of a uniform porous fiber with cylindrical morphology and its controlled winding around a mandrel. This balance also affects the partial fusion at the fiber-fiber contact points, strictly related to the solidification kinetics that was more evident in the case of PHBHHx scaffolds. The different processing parameters optimized for the production of PCL and PHBHHx stents, together with the different physical-chemical properties of the two investigated polymers, led to significant differences in winding angle and fiber diameter, finally determining differences in X-Y pore dimensions and wall thickness between stents with the same N_L. Furthermore, the higher fusion at the fiber-fiber contact points in PHBHHx stents contributed to their lower wall thickness in comparison with PCL stents.

Thermal analysis of processed polymers represents an effective tool to investigate the possible effects of the fabrication conditions (e.g. high temperature, use of organic solvents, UV curing) on different material macromolecular properties. The similarity in thermal degradation profile between unprocessed and processed materials as well as the not significant differences in thermal parameters obtained from DSC second scan suggest that the applied stent manufacturing process did not cause remarkable chemical-physical changes in the molecular structure of the investigated polymers. The three PHBHHx peaks in the first heating DSC thermograms are to be ascribed to the melting of different lamellar crystalline domains formed during polymer solidification and as consequence of heating during thermal analysis [45, 46]. The absence of melting peaks in the second scan curves are due to the experimental rapid cooling from melt that did not allow the formation of crystallinity during PHBHHx solidification. The endothermic peak of PCL samples centered at around 60 °C is ascribable to the melting of polymer crystalline domains and its analysis highlighted that polymer wet-spinning led to high level of polymer crystallinity, corroborating findings from previous studies on PCL processing by CAWS [17, 20, 21].

An intravascular stent is subjected to different mechanical solicitations during insertion and once implanted in the host artery. The longitudinal distortion of a stent, that manifests permanent structural changes such as stent's length reduction and pore change, can occur after initial deployment and during positioning or due to a post-dilatation balloon or intravascular catheter [47-49]. Since a stent longitudinally distorted may predispose to clinical problems, such as restenosis and thrombosis, longitudinal strength is a critical characteristic in the design of a stent. A deployed intravascular stent should possess also enough radial rigidity to keep open the treated artery, and, at the same time, should have a good compliance with the artery wall. In fact, a too rigid stent material can lead to disturbances in normal hemodynamic and wall stress distribution [50, 51]. The stents developed in this study showed longitudinal and radial strength of the same order of magnitude of other polymeric stents reported in literature [38, 52]. However, as expected, their mechanical strength is quite far from those of metallic stents (e.g. cobalt-chromium alloy and nitinol stents) routinely employed in the clinical practice [48, 53]. Possible strategies to enhance their radial and axial response involve optimizing stent design, as well as tuning polymeric matrix microporosity and fusion at contact points by acting on different phase inversion parameters, as previously discussed. The investigation of elasticity retention properties was aimed at assessing the ability of the stents to recover their initial shape and sizes when subjected to axial or radial compression. In general, the stents showed good elasticity being

able to recover their initial size for axial or radial deformations even larger than 30%. In particular, PHBHHx stents showed remarkable radial elasticity, with a full elastic recovery for applied compressive strain values up to 70 %.

In the clinical practice, stents intended for small caliber blood vessels are usually delivered at the injure site by means of a balloon-assisted expansion procedure. To this aim, the stent is crimped onto an angioplasty balloon in a non-expanded configuration and then is permanently expanded to the vessel lumen size. Polymeric stents are generally expanded to at least twice their initial diameter displaying a viscoelastic behavior characterized by a plastic and an elastic deformation component, the latter being recovered instantaneously after balloon deflation. The extent of elastic recovery can be controlled in a certain range by acting on different factors including tunable material properties (e.g. T_g) or expansion procedure variables (e.g. strain rate, temperature and duration of stress imposition) [54]. Effective approaches followed to minimize elastic recoil after balloon expansion have involved the development of complex stent configurations, like in the case of laser cut PLLA stents with a definite slanted-slit pattern [55] or PLLA/poly(4-hydroxybutyrate) blend stents with a slotted-tube design [56]. A different strategy is based on conferring elastic memory properties to the stent, usually through a temperature conditioning process, in such a way that under physiological conditions the polymer molecular mobility increases leading to tube expansion to a predefined diameter. As an example, the clinically-approved Igaki-Tamai stent requires to be heated to 80 °C in order to self-expand its zig-zag patterned PLLA filament structure through a balloon-assisted procedure [11]. Future studies should address the expandability strategy of the developed PHBHHx and PCL stents. Considering the relatively low T_g of these two polymers, well below 37 °C, it is reasonable to expect a significant plastic deformation upon their balloon expansion. However, because their marked elastic behavior, as also demonstrated in the compressive characterization carried out in this study, it is likely that they will show an appreciable elastic recoil after deployment. Investigation of different stent design aspects, such as polymeric strut pattern and tailored fusion at the contact points to create a cohesive structure with a proper plastic response to deformation, is recommended in order to optimize stents expansion properties. To this end, the versatility of the developed CAWS technique in terms of stent design freedom and reproducibility should be further tested and optimized.

As shown by *in vitro* investigations, the developed stents were able to support endothelial cells adhesion and proliferation, and demonstrated a low level of thrombogenicity in comparison to glass, employed as positive reference. Glass, together with silicone or latex rubber, are the materials most often employed as positive control for thrombogenicity, while poly(vinyl chloride) and polyethylene are commonly used as reference negative materials. In general, the polymers more extensively investigated and employed for cardiovascular applications react mildly as compared to stenting metals such as stainless steel or nitinol alloys [57]. Although the heterogeneous experimental data sets available in the current literature on comparative thrombogenicity of metals, strictly related to differences in material surface chemistry and topography that result from various alloys compositions and surface treatment protocols, nitinol alloys and stainless steells generally result in fibrinogen adsorption values of the same order of magnitude, and in some cases higher, in comparison with glass [58]. The excellent results in terms of thromboresistivity achieved in this study may be attributed to the stents structure. The relatively high pore size of the stent wall, in the order of hundreds of micrometers, would probably offer a reduced surface for fibrinogen deposition, thus preventing the activation of the cascade and platelet activation for the formation of the blood clot [59, 60].

The treatment of polyesters with NaOH have been investigated by a number of studies as a means to enhance surface hydrophilicity and consequently to achieve a better interaction with cells [61-63]. As an example, Serrano *et al*. demonstrated that NaOH treatment of PCL films leads to improved adhesion and proliferation of pig vascular endothelial and smooth muscle cells [61]. However, the preliminary results obtained in this study suggest that the treatment with NaOH does not improve the susceptibility to endothelialization of the developed stents. On the other hand, the NaOH-treated PHBHHx stents demonstrated the best performance in terms of thromboresistivity.

Conclusions

The main result attained during this study was the development of a novel CAWS approach allowing for the layer-by-layer fabrication of tubular PHBHHx and PCL structures employable as stents for small diameter blood vessels treatment. The developed technique showed a great versatility in the customization of stent composition, dimensions and wall microporosity. As shown by thermal characterization, material processing did not affect significantly the chemical-physical properties of the materials. Mechanical characterization demonstrated that stent axial and radial properties could be tuned in a certain range by acting on compositional and structural parameters. Overall, PHBHHx stents demonstrated good radial elasticity, while

PCL stents showed mechanical strength along both radial and axial direction comparable with other stents made of the same polymer but produced by means of other techniques. The developed stents well supported *in vitro* endothelial cells proliferation and showed excellent thromboresistivity.
The present study opens new possibilities for the employment of a novel fabrication approach allowing to customize stent micro- and macro-structural features and mechanical properties. Future work will address the *ex vivo* and *in vivo* assessment of the developed stents potential as biodegradable intravascular implants for small caliber blood vessel treatment.

Acknowledgments
The reported research activity was supported by the European Eranet+ project, BI-TRE - BIophotonic technologies for Tissue Repair (2014-2016). PHBHHx was kindly supplied by Prof. Guo-Qiang Chen of Tsinghua University (Beijing, China) within the framework of the EC-Funded project Hyanji Scaffold in the People Program of the 7FP (2010-2013). Dr. M. Gazzarri and Dr. C. Bartoli are acknowledged for their kind contribution during biological characterization. Dr. Randa Ishak is acknowledged for her support in recording SEM images. The authors declare that there is no conflict of interest.

References
1. Serruys PW, et al. 1994 A Comparison of Balloon-Expandable-Stent Implantation with Balloon Angioplasty in Patients with Coronary Artery Disease *New Engl. J. Med.* **331** 489-95
2. Waksman R 2006 Biodegradable Stents: They Do Their Job and Disappear *J Invasive Cardiol* **18** 70-4
3. Alexy RD, Levi DS 2013 Materials and Manufacturing Technologies Available for Production of a Pediatric Bioabsorbable Stent *BioMed Res. Int.* **2013** 11
4. Bangalore S, Toklu B, Amoroso N, Fusaro M, Kumar S, Hannan E, Faxon D, Feit F 2013 Bare metal stents, durable polymer drug eluting stents, and biodegradable polymer drug eluting stents for coronary artery disease: mixed treatment comparison meta-analysis *BMJ* **347** 6625-45
5. Heublein B, Rohde R, Kaese V, Niemeyer M, Hartung W, Haverich A 2003 Biocorrosion of magnesium alloys: a new principle in cardiovascular implant technology? *Heart* **89** 651-6
6. Bolz A, Popp T 2001 Implantable, bioresorbable vessel wall support, in particular coronary stent US6287332 B1
7. Klocke B, Diener T, Fringes M, Harder C 2009 Degradable metal stent having agent containing coating US20090030507
8. Erbel R, et al. 2007 Temporary scaffolding of coronary arteries with bioabsorbable magnesium stents: a prospective, non-randomised multicentre trial *Lancet* **369** 1869-75
9. Martinez AW, Chaikof EL 2011 Microfabrication and nanotechnology in stent design *Nanomed. Nanobiotechnol.* **3** 256-68
10. Tamai H, et al. 2000 Initial and 6-month results of biodegradable poly-l-lactic acid coronary stents in humans *Circulation* **102** 399-404
11. Nishio S, et al. 2012 Long-Term (>10 Years) Clinical Outcomes of First-in-Human Biodegradable Poly-l-Lactic Acid Coronary Stents: Igaki-Tamai Stents *Circulation* **125** 2343-53
12. Gogas BD, Farooq V Fau - Onuma Y, Onuma Y Fau - Serruys PW, Serruys PW 2012 The ABSORB bioresorbable vascular scaffold: an evolution or revolution in interventional cardiology? *Hellenic J. Cardiol.* **53** 301-9
13. Flege C, et al. 2013 Development and characterization of a coronary polylactic acid stent prototype generated by selective laser melting *J. Mater. Sci. - Mater. Med.* **24** 241-55
14. Mota C, Puppi D, Chiellini F, Chiellini E 2015 Additive manufacturing techniques for the production of tissue engineering constructs *J. Tissue Eng. Regen. Med.* **9** 174-90
15. Puppi D, Zhang X, Yang L, Chiellini F, Sun X, Chiellini E 2014 Nano/microfibrous polymeric constructs loaded with bioactive agents and designed for tissue engineering applications: a review *J. Biomed. Mater. Res. B Appl. Biomater.* **102** 1562-79
16. Puppi D, Mota C, Gazzarri M, Dinucci D, Gloria A, Myrzabekova M, Ambrosio L, Chiellini F 2012 Additive manufacturing of wet-spun polymeric scaffolds for bone tissue engineering *Biomed. Microdevices* **14** 1115-27
17. Mota C, Puppi D, Dinucci D, Gazzarri M, Chiellini F 2013 Additive manufacturing of star poly(ε-caprolactone) wetspun scaffolds for bone tissue engineering applications *J. Bioact. Compat. Polym.* **28** 320-40
18. Mota C, Wang SY, Puppi D, Gazzarri M, Migone C, Chiellini F, Chen GQ, Chiellini E 2017 Additive manufacturing of poly[(R)-3-hydroxybutyrate-co-(R)-3-hydroxyhexanoate] scaffolds for engineered bone development *J Tissue Eng Regen Med* **11** 175-86
19. Dini F, et al. 2015 Tailored star poly (ε-caprolactone) wet-spun scaffolds for in vivo regeneration of long bone critical size defects *J. Bioact. Compat. Polym.* **31** 15-30
20. Puppi D, Piras AM, Pirosa A, Sandreschi S, Chiellini F 2016 Levofloxacin-loaded star poly(ε-caprolactone) scaffolds by additive manufacturing *J. Mater. Sci. - Mater. Med.* **27** 1-11

21. Puppi D, Migone C, Grassi L, Pirosa A, Maisetta G, Batoni G, Chiellini F 2016 Integrated three-dimensional fiber/hydrogel biphasic scaffolds for periodontal bone tissue engineering *Polym. Int.* **65** 631-40
22. Puppi D, Migone C, Morelli A, Bartoli C, Gazzarri M, Pasini D, Chiellini F 2016 Microstructured chitosan/poly(γ-glutamic acid) polyelectrolyte complex hydrogels by computer-aided wet-spinning for biomedical three-dimensional scaffolds *J. Bioact. Compatible Polym.* **31** 531-49
23. Chiellini F, Puppi D, Piras AM, Morelli A, Bartoli C, Migone C 2016 Modelling of pancreatic ductal adenocarcinoma in vitro with three-dimensional microstructured hydrogels *RSC Adv.* **6** 54226-35
24. Puppi D, Pirosa A, Morelli A, Chiellini F 2016 Design, fabrication and characterization of tailored poly[(R)-3-hydroxybutyrate-*co*-(R)-3-hydroxyexanoate] scaffolds by Computer-aided Wet-spinning *Rapid Prototyping J.* In press
25. Mei N, Zhou P, Pan L, Chen G, Wu C, Chen X, Shao Z, Chen G 2006 Biocompatibility of poly (3-hydroxybutyrate-co-3-hydroxyhexanoate) modified by silk fibroin *J Mater Sci Mater Med* **17** 749-58
26. Zhao K, Deng Y, Chun Chen J, Chen G-Q 2003 Polyhydroxyalkanoate (PHA) scaffolds with good mechanical properties and biocompatibility *Biomaterials* **24** 1041-5
27. Puppi D, Chiellini F, Dash M, Chiellini E 2011 Biodegradable Polymers for Biomedical Applications. In: Felton GP, editor. Biodegradable Polymers: Processing, Degradation & Applications. New York: Nova Science Publishers. p. 545-60.
28. Woodruff MA, Hutmacher DW 2010 The return of a forgotten polymer—Polycaprolactone in the 21st century *Prog. Polym. Sci.* **35** 1217-56
29. Brown TD, Slotosch A, Thibaudeau L, Taubenberger A, Loessner D, Vaquette C, Dalton PD, Hutmacher DW 2012 Design and Fabrication of Tubular Scaffolds via Direct Writing in a Melt Electrospinning Mode *Biointerphases* **7** 13
30. Serrano M, Pagani R, Vallet-Regi M, Pena J, Comas J, Portoles M 2009 Nitric oxide production by endothelial cells derived from blood progenitors cultured on NaOH-treated polycaprolactone films: A biofunctionality study *Acta Biomater.* **5** 2045-53
31. Dalton PD, Shoichet MS 2001 Creating porous tubes by centrifugal forces for soft tissue application *Biomaterials* **22** 2661-9
32. Wang S, Cai Q, Hou J, Bei J, Zhang T, Yang J, Wan Y 2003 Acceleration effect of basic fibroblast growth factor on the regeneration of peripheral nerve through a 15-mm gap *J Biomed Mater Res A* **66A** 522-31
33. Detta N, Errico C, Dinucci D, Puppi D, Clarke DA, Reilly GC, Chiellini F 2010 Novel electrospun polyurethane/gelatin composite meshes for vascular grafts *J. Mater. Sci. - Mater. Med.* **21** 1761-9
34. Zheng Y, et al. 2012 In vitro microvessels for the study of angiogenesis and thrombosis *Proc. Natl. Acad. Sci. U. S. A.* **109** 9342-7
35. Xu C, Zhang Z, Christensen K, Huang Y, Fu J, Markwald RR 2014 Freeform Vertical and Horizontal Fabrication of Alginate-Based Vascular-Like Tubular Constructs Using Inkjetting *J. Manuf. Sci. Eng.* **136** 061020-
36. Jingyuan Y, Yong H, Douglas BC 2013 Laser-assisted printing of alginate long tubes and annular constructs *Biofabrication* **5** 015002
37. Flege C, et al. 2013 Development and characterization of a coronary polylactic acid stent prototype generated by selective laser melting *J Mater Sci Mater Med* **24** 241-55
38. Brown TD, Slotosch A, Thibaudeau L, Taubenberger A, Loessner D, Vaquette C, Dalton PD, Hutmacher DW 2012 Design and Fabrication of Tubular Scaffolds via Direct Writing in a Melt Electrospinning Mode *Biointerphases* **7** 1-16
39. Jungst T, Muerza-Cascante ML, Brown TD, Standfest M, Hutmacher DW, Groll J, Dalton PD 2015 Melt electrospinning onto cylinders: effects of rotational velocity and collector diameter on morphology of tubular structures *Polym. Int.* **64** 1086-95
40. ASTM Standard F2792–12a. 2012; Standard terminology for additive manufacturing technologies; DOI: 10.1520/F2792–12A; www.astm.org
41. Gibson I, Rosen D, Stucker B. Additive Manufacturing Technologies: Rapid Prototyping to Direct Digital Manufacturing. Gibson I, Rosen D, Stucker B, editors. New York Heidelberg Dordrecht London: Springer; 2010.
42. Puppi D, Chiellini F 2017 Wet-spinning of Biomedical Polymers: from Single Fibers Production to Additive Manufacturing of 3D Scaffolds *Polym. Int.* doi: 10.1002/pi.5332
43. Sun H, Mei L, Song C, Cui X, Wang P 2006 The in vivo degradation, absorption and excretion of PCL-based implant *Biomaterials* **27** 1735-40
44. Chen G-Q, Wu Q 2005 The application of polyhydroxyalkanoates as tissue engineering materials *Biomaterials* **26** 6565-78
45. Yang H-X, Sun M, Zhou P 2009 Investigation of water diffusion in poly(3-hydroxybutyrate-co-3-hydroxyhexanoate) by generalized two-dimensional correlation ATR–FTIR spectroscopy *Polymer* **50** 1533-40
46. Ding C, Cheng B, Wu Q 2011 DSC analysis of isothermally melt-crystallized bacterial poly(3-hydroxybutyrate-co-3-hydroxyhexanoate) films *J. Therm. Anal. Calorim.* **103** 1001-6
47. Hanratty C, Walsh S 2011 Longitudinal compression: a "new" complication with modern coronary stent platforms-time to think beyond deliverability *EuroIntervention* **7** 872-7
48. Ormiston JA, Webber B, Webster MW 2011 Stent longitudinal integrity bench insights into a clinical problem. *JACC Cardiovasc. Interv.* **4** 1310-7

49. Pitney M, Pitney K, Jepsom N 2011 Major stent deformation/pseudofracture of 7 crown Endeavor/Micro Driver stent platform: incidence and causative factors *EuroIntervention* **7** 256-62
50. Berry JL, Moore J, Newman VS, Routh WD 1997 In vitro flow visualization in stented arterial segments *J. Vasc. Invest.* **3** 63-8
51. Rolland PH, Mekkaoui C, Vidal V, Berry JL, Moore JE, Moreno M, Amabile P, Bartoli JM 2004 Compliance Matching Stent Placement in the Carotid Artery of the Swine Promotes Optimal Blood Flow and Attenuates Restenosis *Eur. J. Vasc. Endovasc. Surg.* **28** 431-8
52. Liu S, Chiang F, Hsiao C, Kau Y, Liu K 2010 Fabrication of balloon-expandable self-lock drug-eluting polycaprolactone stents using micro-injection molding and spray coating techniques *Ann Biomed Eng* **38** 3185-94
53. Mechanical Properties of Nitinol Stents and Stent-grafts: Comparison of 6 mm Diameter Devices. [July 2016]; Available from: www.goremedical.com.
54. Venkatraman S, Boey F, Lao LL 2008 Implanted cardiovascular polymers: Natural, synthetic and bio-inspired *Prog. Polym. Sci.* **33** 853-74
55. Grabow N, Schlun M, Sternberg K, Hakansson N, Kramer S, Schmitz K-P 2005 Mechanical Properties of Laser Cut Poly(L-Lactide) Micro-Specimens: Implications for Stent Design, Manufacture, and Sterilization *J. Biomech. Eng.* **127** 25-31
56. Grabow N, Bünger CM, Schultze C, Schmohl K, Martin DP, Williams SF, Sternberg K, Schmitz K-P 2007 A Biodegradable Slotted Tube Stent Based on Poly(l-lactide) and Poly(4-hydroxybutyrate) for Rapid Balloon-Expansion *Ann. Biomed. Eng.* **35** 2031-8
57. van Oeveren W 2013 Obstacles in Haemocompatibility Testing *Scientifica* **2013** 14
58. Shabalovskaya S, Anderegg J, Van Humbeeck J 2008 Critical overview of Nitinol surfaces and their modifications for medical applications *Acta Biomater.* **4** 447-67
59. Mohan CC, Chennazhi KP, Menon D 2013 In vitro hemocompatibility and vascular endothelial cell functionality on titania nanostructures under static and dynamic conditions for improved coronary stenting applications *Acta Biomater.* **9** 9568-77
60. Seyfert UT, Biehl V, Schenk J 2002 In vitro hemocompatibility testing of biomaterials according to the ISO 10993-4 *Biomol. Eng.* **19** 91-6
61. Serrano MC, Portolés MT, Vallet-Regí M, Izquierdo I, Galletti L, Comas JV, Pagani R 2005 Vascular Endothelial and Smooth Muscle Cell Culture on NaOH-Treated Poly(ε-caprolactone) Films: A Preliminary Study for Vascular Graft Development *Macromol. Biosci.* **5** 415-23
62. Yeo A, Wong WJ, Khoo HH, Teoh SH 2010 Surface modification of PCL-TCP scaffolds improve interfacial mechanical interlock and enhance early bone formation: An in vitro and in vivo characterization *J Biomed Mater Res A* **92** 311-21
63. Drevelle O, Bergeron E, Senta H, Lauzon M-A, Roux S, Grenier G, Faucheux N 2010 Effect of functionalized polycaprolactone on the behaviour of murine preosteoblasts *Biomaterials* **31** 6468-76